World Academy of Science, Engineering and Technology
International Journal of Energy and Power Engineering
Vol:10, No:6, 2016

Effects of Turbulence Penetration on Valve Leakage in Nuclear Reactor Coolant System

Gupta Rajesh, Paudel Sagar, Sharma Utkarsh, Singh Amit Kumar

Abstract**—**Thermal stratification has drawn much attention because of the malfunctions at various nuclear plants in U.S.A that raised significant safety concerns. The concerns due to this phenomenon relate to thermal stresses in branch pipes connected to the reactor coolant system piping. This stress limits the lifetime of the piping system, and even leading to penetrating cracks. To assess origin of valve damage in the pipeline, it is essential to determine the effect of turbulence penetration on valve leakage; since stratified flow is generally generated by turbulent penetration or valve leakage. As a result, we concluded with the help of coupled fluent-structural analysis that the pipe with less turbulence has less chance of failure there by requiring less maintenance.

Keywords**—**Reactor coolant system, thermal stratification, turbulent penetration, coupled fluent-structural analysis, Von Mises stress.

I. Introduction

THE problem of thermal stratification came into existence in the period of initial 1980s. Cracks due to stratification were found in the US, France, Belgium, Finland and Japan power plants [1]. Due to series of coolant system failure in US, U.S. Nuclear Reactor Corporation released a report for the pipe crack which first talked about thermal stratification in pipes [2]. There was an event involving cracking and leaking of a pipe elbow due to thermal fatigue in the letdown system of a PWR. There are two well-known factors which provoke thermal stratification in this system. The first factor is the turbulent penetration of hot coolant from the reactor coolant system to the branch line. RCS flow is more rapid and relatively hot compared to the branch line flow so it is possible to produce turbulent penetration near the branch. The second factor is leakage through damage in the first closed valve. For instance, in 1996, due to the nonlinear temperature distribution caused by valve leakage, a through-wall crack developed in a horizontal pipe of the SIS in Dampierr Unit 1 in Japan [3]. Piping becomes "thinner" due to combined effects of flow velocity together with unfavorable materials and water chemistry. This phenomenon is called wall thinning, or flow-assisted corrosion [4]. Thermal fatigue due to stratification and mixing of hot and cold water is a recurring phenomenon, but with a relatively low frequency. There were also reports on cracks and leaks caused by periodic mixing of hot and cold water (thermal fatigue) [2]. The valves are used for isolation purposes and for flow regulation. Many safety systems have isolation valves that may change their position during challenging transient conditions. Pressure locking due to thermal binding is the term used when the liquid inside the valve body heats up and pressurizes the valve discs [4]. Under these conditions, differential thermal expansion of the pipe metal can cause the pipe to deflect significantly. Unexpected piping movements are highly undesirable because of the potential for high piping stress that may exceed design limits for fatigue and stress. The problem can become more acute when piping expansion is restricted, such as through contact with pipe whip restraints. Plastic deformation can result, which can lead to high local stress, low cycle fatigue and functional impairment of the line [1]. Metallic components subjected to thermal cycling/thermal fatigue may fail in one of the way cracks appear first on the hot zone of the component and may eventually propagate through the section. This is the most common type of failure observed in grey cast irons and other brittle materials [5]. Afterwards several researches were carried out in the field to analyze the effect of both turbulence penetration and valve leakage in the pipe damage. But the main cause of valve leakage has not been pointed in previous studies between chemical corrosion or thermal corrosion.

Our study is aimed to decipher the effect of turbulence penetration on valve deterioration in short term effect. For that we have considered the valve as our domain of study to apply transient equation and point the critical points where Von Mises stress is maximum. Since there is a linear relationship between the stresses and temperature, the distribution of the Von Mises stresses is similar to that of the temperature [6]. Aiming to improve the knowledge on thermally stratified flow, we focused our study on long term fatigue destruction of valve due to turbulence penetration and increase life management and safety in nuclear reactors, numerical problems has been set up by us to simulate the problem. The software used consists of ANSYS structural and ANSYS FLUENT for combined solid- fluid domain analysis.

II. Mathematical Formulation

Fig. 1 shows the three dimensional view of the reactor coolant system along with safety injection branch pipe. The safety injection branch pipe is connected to the upper reactor coolant system cold leg. There is a valve at the end of safety injection branch pipe and is closed under normal operating condition. Cold coolants are kept after the valve and are used in order to pressurize the reactor coolant system under depressurization for the purpose of safety aspects.

Gupta Rajesh is with the Maulana Azad National Institute of Technology, Bhopal (M.P.)-462007, India (e-mail: gupta_rjp@yahoo.co.in).

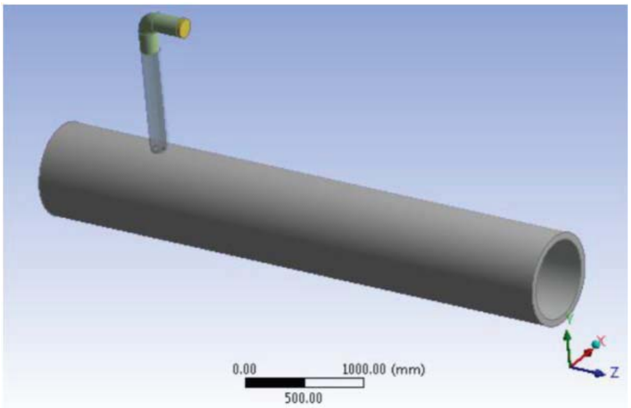

Fig. 1 Physical Model

A. Meshing

For fluid domain, hexahedral and tetrahedral mesh has been set up with inflation while for solid domain, tetrahedral mesh setting has been applied with inflation on the inner surface of pipe. The SIS pipe has been allotted hexahedral and others tetrahedral because hexahedral mesh are much more accurate but takes longer processing time and SIS pipe is the main domain of our study. Then, the material is applied on pipe as structural steel and fluid as water liquid.

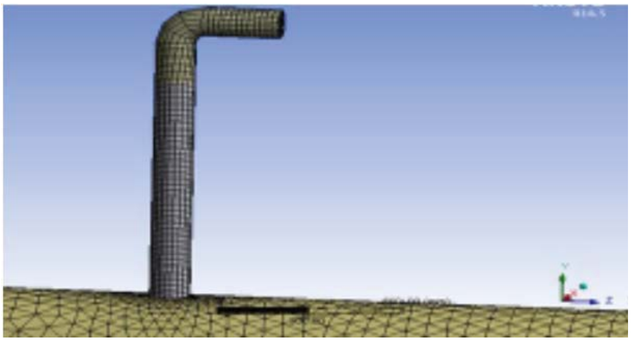

Fig. 2 Meshed model

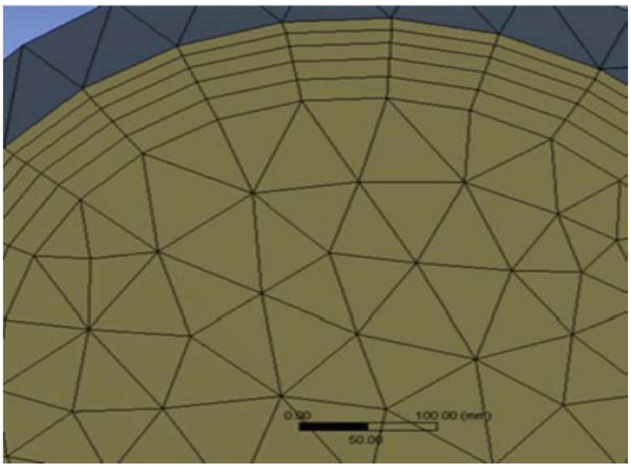

Fig. 3 Inflation on boundary of solid and fluid

TABLE I
MESH STATISTICS

Total nodes	41062
Total elements	103842
Avg. orthogonal quality	0.8827849838

A turbulence model is a computational procedure to close the system of mean flow equations. For most engineering applications it is unnecessary to resolve the details of the turbulent fluctuations [7]. CFD analysis can give experimental analysis a run for its money in many cases of detrimental studies [8]. Turbulence models allow the calculation of the mean flow without first calculating the full time-dependent flow field. We only need to know how turbulence affected the mean flow and in particular we need expressions for the Reynolds stresses [9]. Equation (1) is the general equations for the flow and (4)-(8) are common turbulence modeling equation as given below:

B. Governing Equations

$$\frac{\partial}{\partial t}\int \rho\phi dv + \oint \rho\phi v.dA = \oint \Gamma_\phi \nabla\phi.dA + \int S_\phi dv \quad (1)$$

where field variable $(\phi) = h$ for energy equation, Γ_ϕ is diffusion coefficient, S_ϕ is the heat generation per unit volume.

C. Continuity Equation

$$\frac{\partial\rho}{\partial t} + \frac{\partial(\rho u)}{\partial x} + \frac{\partial(\rho v)}{\partial y} + \frac{\partial(\rho w)}{\partial z} = 0 \quad (2)$$

where ρ is the density and u, v & w represents fluid velocity in x, y and z directions respectively.

D. Momentum Equation

$$\rho\frac{Du}{Dt} = \rho b_x + \frac{\partial\tau_{xx}}{\partial x} + \frac{\partial\tau_{yx}}{\partial y} + \frac{\partial\tau_{zx}}{\partial z} = 0 \quad (3)$$

where the term on left hand term represents the rate of increase of x-momentum per unit volume of the fluid particle and τ_{xx}, τ_{yx}, τ_{zx} are the stress components and ρb_x is the body force due to gravity.

E. Turbulence Modelling Equation

$$\tau_{ij} - \rho\overline{\acute{u}_i\acute{u}_j} = \mu_T\left(\frac{\partial U_i}{\partial x_j} + \frac{\partial U_j}{\partial x_i}\right) \quad (4)$$

$$K = \frac{1}{2}(U^2 + V^2 + W^2) \quad (5)$$

$$k = \frac{1}{2}\left(\overline{\acute{u}^2} + \overline{\acute{v}^2} + \overline{\acute{w}^2}\right) \quad (6)$$

$$k(t) = K + k \quad (7)$$

where **K** is mean kinetic energy, **k** is turbulent kinetic energy and **k (t)** is instantaneous kinetic energy of a turbulent flow.

$$\mu_t = \rho C_\mu \frac{k^2}{\varepsilon} \quad (8)$$

where μ_t is turbulent viscosity. We have used realizable *k*-ε model for the Reynolds Average Navier Stokes (RANS) equation solution. To find k and ε, equation of kinetic energy *k* is composed of mean and turbulent kinetic energy; and ε equation is similar to kinetic energy and they are listed in (9)-(13) [9].

$$\frac{\partial \varepsilon}{\partial t} + U_i \frac{\partial \varepsilon}{\partial x_i} = \frac{\partial}{\partial x_i}\left[\left(\nu + \frac{\nu_T}{\sigma_\varepsilon}\right)\frac{\partial \varepsilon}{\partial x_i}\right] + C_{\varepsilon 1} f_{\varepsilon 1} \frac{\varepsilon}{k} P_k - C_{\varepsilon 2} f_{\varepsilon 2} \frac{\varepsilon^2}{k} + R \quad (9)$$

$$\mu_t = \rho C_\mu \frac{k^2}{\varepsilon}, C_\mu = \frac{1}{A_0 + A_i \frac{U^* k}{\varepsilon}} \quad (10)$$

$$U^* = \sqrt{S_{ij} S_{ij} + \Omega_{ij} \Omega_{ij}} \quad (11)$$

$$A_0 = 4.04 \;\; , A_s = \sqrt{6}\cos\phi , \phi = \frac{1}{3}\cos^{-1}\left(\sqrt{6}W\right) \quad (12)$$

$$W = \frac{S_{ij} S_{ji} S_{ki}}{\tilde{S}}, \tilde{S} = \sqrt{S_{ij} S_{ij}} \quad (13)$$

TABLE II
STANDARD MODEL COEFFICIENTS

$C\varepsilon 1$	$C\varepsilon 2$	σk	$\sigma\varepsilon$	$C\mu$	κ
1.47	1.83	1.0	1.56	0.09	0.41

As solver in ANSYS, we have used SIMPLE algorithm. The u, v, w, and p fields are solved separately. Coupling between these field variables is achieved via velocity and pressure corrections. Convergence occurs when the residuals for each of the equations is reduced to a value below a tolerance. The algorithm is iterative. There are many different ways to implement this, but second-order upwind with limiters is one of the more popular numerical schemes because of its combination of accuracy and stability. Grid independency study was performed to support our result's accuracy; the result of which are given below:

F. Grid Independency Test

TABLE III
GRID INDEPENDENCE AT GLANCE

No. of elements	Valve temp. (K)	Max % difference
29297	458.26	
48797	457.05	0.00264
79782	456.04	0.00149
169924	456.72	0.00075

G. Boundary Conditions

The safety injection system (SIS) is one of those branch lines which inject safety fluid in the reactor chamber. This line is connected to the cold leg of the RCS to supply water steam and remove excessive heat in the event of an accidental depressurization of the RCS. Therefore, during normal operation, all valves in the SIS are closed to maintain the SIS cold coolant stagnantly. RCS flow is more rapid and relatively hot compared to the branch line flow so it is possible to produce turbulent penetration near the branch.

Two different types of SIS piping were considered in this study. The SIS pipe is connected to the upper RCS cold leg and all valves in these lines are closed during normal and startup operating conditions. The geometric features and hydraulic conditions of each SIS pipe are presented in Table IV. Generally, it is difficult to generate turbulence penetration in a pipe which has a long vertical line and a small diameter. Therefore, the effects of geometric features on the thermal stratification phenomenon were analyzed qualitatively based on these popular views [6].

In this research, all valves were simplified to a valve disk whose thickness was assumed to be uniform. All outer surfaces of the piping were assumed to be adiabatic and a no-slip condition was applied to all inner surfaces of the piping. The gauge pressure over the outlet was assumed to be zero. The end of each branch line was assumed to be isolated and to have a 322 K low temperature wall.

TABLE IV
INPUT PARAMETERS

Input parameters	Value
I.D. pipe(RCS)	699mm
I.D. pipe (Branch)	132mm
Thickness pipe(RCS)	59mm
Thickness pipe (Branch)	18mm
Valve thickness	36mm
Vertical Tube length	Type I – 1000mm Type II - 500 mm
Initial temp. (pipe wall)	322 K
Initial temp. (fluid)	567 K
Mass flow rate	4486 kg/sec.

III. ANALYSIS METHODOLOGY

For conducting coupled fluent-structural analysis, we have made some assumptions. Unsteady state, incompressible and three dimensional flows is flowing in the reactor coolant system. Radiation heat transfer and its effect are neglected. Conjugate heat transfer analysis is carried out in to CFD analysis in order to take into the account of interaction between pipe wall and fluid. The Reynolds's number of the flow in the safety injection branch pipe is estimated to be in the turbulent region.

Momentum and energy equation has been activated with transient turbulent flow condition. Realizable *k*-ε model has been activated for the flow in this step since we need the temperature distribution around the pipe wall. For material setting, the fluent has only structural steel which is close to the actual material used in nuclear reactor that is ASMI SUS304 [6] and as fluid material we choose liquid water.

SIMPLE algorithm was applied in the solver with second order upwind scheme for momentum, turbulent kinetic energy and turbulent dissipation energy. Last step is the main step of the analysis in which we decide the processing time of our analysis according to the requirement of the problem and/or the memory of the processor. Time step size, time step number, iterations and maximum iterations are regulated in this step of analysis. Transient analysis is applied first order implicit method. Convergence occurs when the residuals for each of the equations is reduced to a value below a tolerance value of the order of 10^{-4}. To satisfy the convergence criterion, iterations of less than 10 times per time step were needed. After getting the solution of temperature distribution inside the pipe, we shift to the transient structural window as shown before. The temperature profile is imported from FLUENT to structural and setting is applied for Von-Mises stresses in the pipe. The two types of models with variable length are used to predict the results for the temperature distribution.

IV. Results and Discussions

The results after 1000 sec. seemed to diverge and therefore were neglected from the computation. The results obtained by ANSYS were devised into two forms: graphical and figurative. Figs. 5-7 show type I tube velocity profile, temperature profile and Von Misses stresses at the inner wall of valve at 150 and 300 sec.

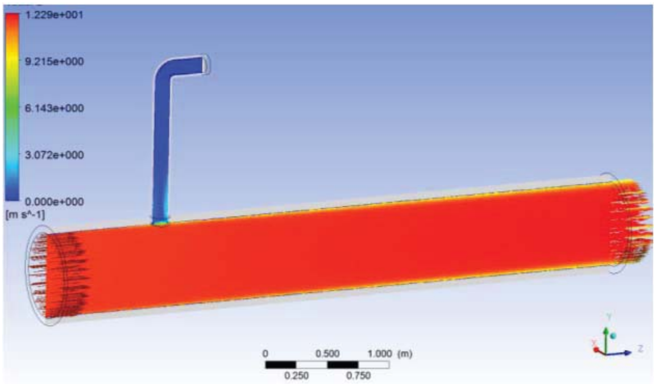

Fig. 4 Velocity distribution in Type I pipe

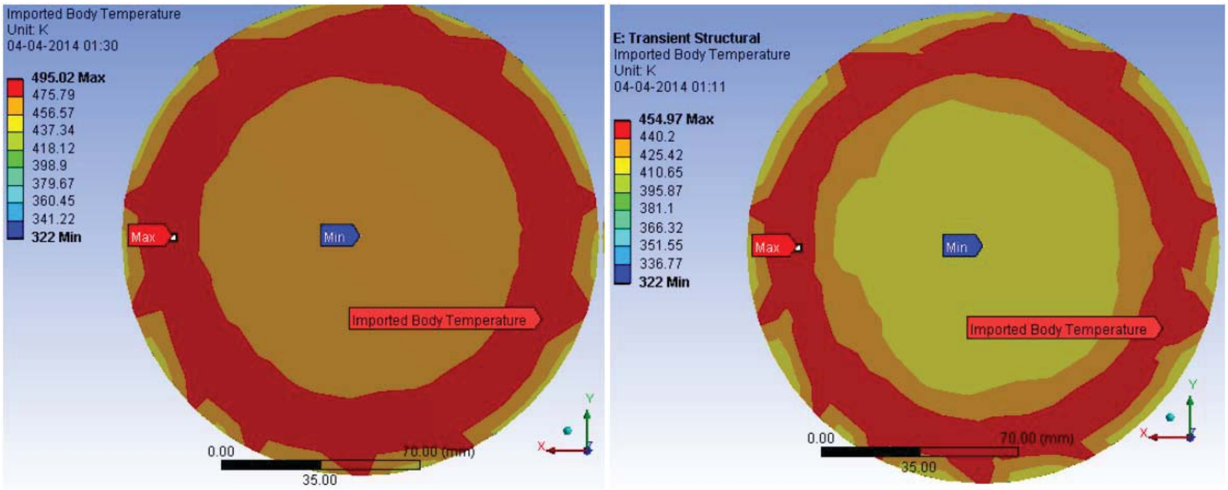

Fig. 5 Temperature distribution in type I

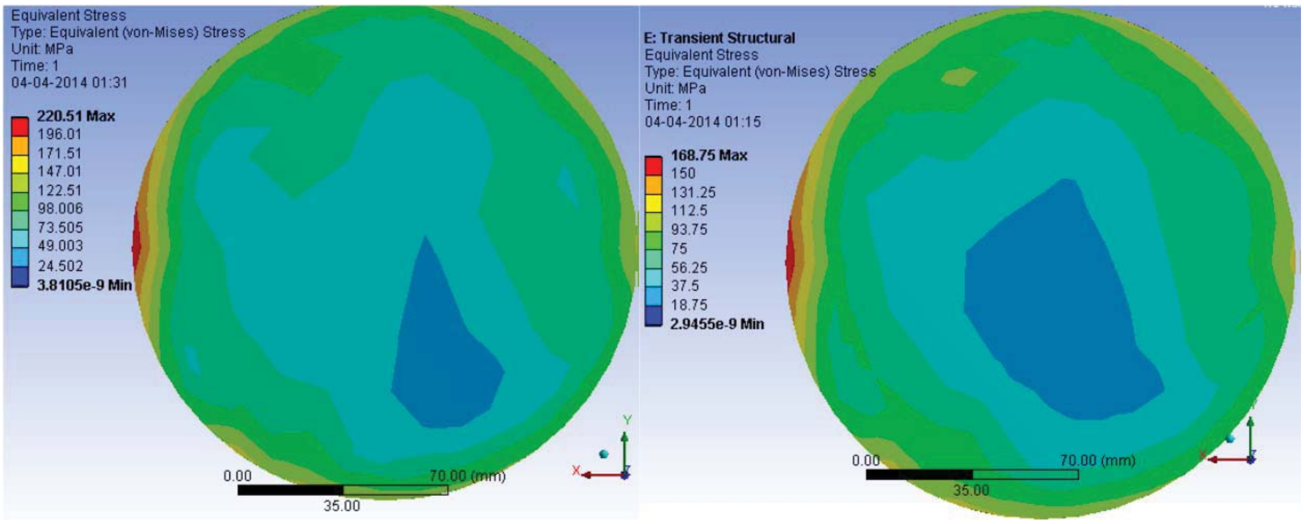

Fig. 6 Stress distribution in type I

Fig. 4 represents the velocity vectors in the reactor coolant system as well as in safety injection pipe. Due to geometrical features, there exists the turbulent penetration in the safety injection pipe with the minimum velocity of 1.4 m/s. Strong swirl flow is obtained in the first branch point due to the fact that large pressure difference was induced by the geometric design and features of the safety injection pipe system.

Figs. 5 and 6 show the temperature as well as stress distribution in type I SIS piping at a specific time. The maximum temperature difference of 48 K is obtained in the inner wall of the valve at first 50 s. However, with the time, the temperature difference decreases and attains the steady state after 1000 seconds.

Fig. 6 shows that the stresses developed on the inner wall of the valve have a maximum value at 9 o'clock position in first 150 s. The value of this maximum stress at that particular position increases with the increment of time step.

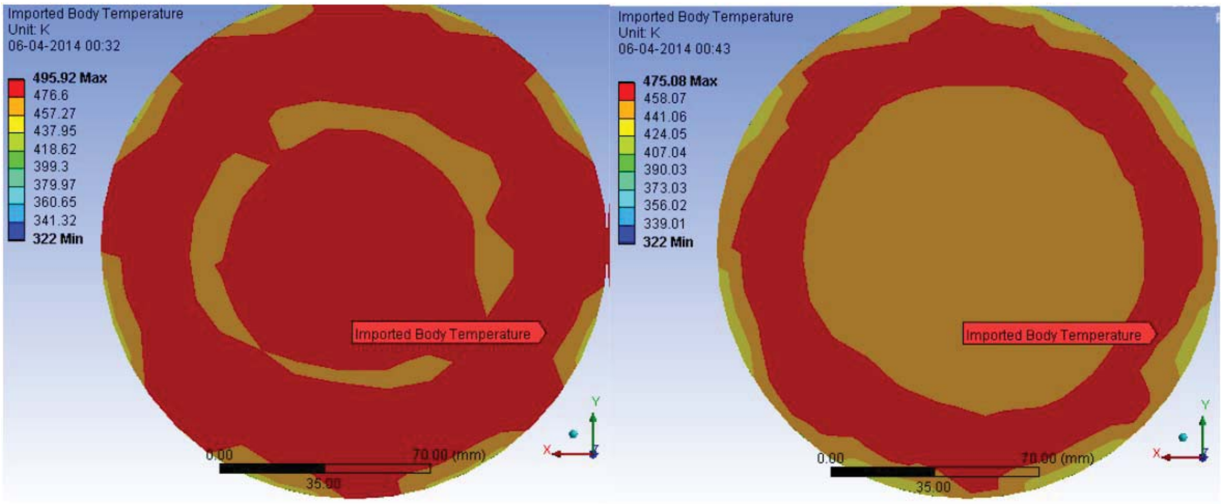

Fig. 7 Temperature distribution in type II

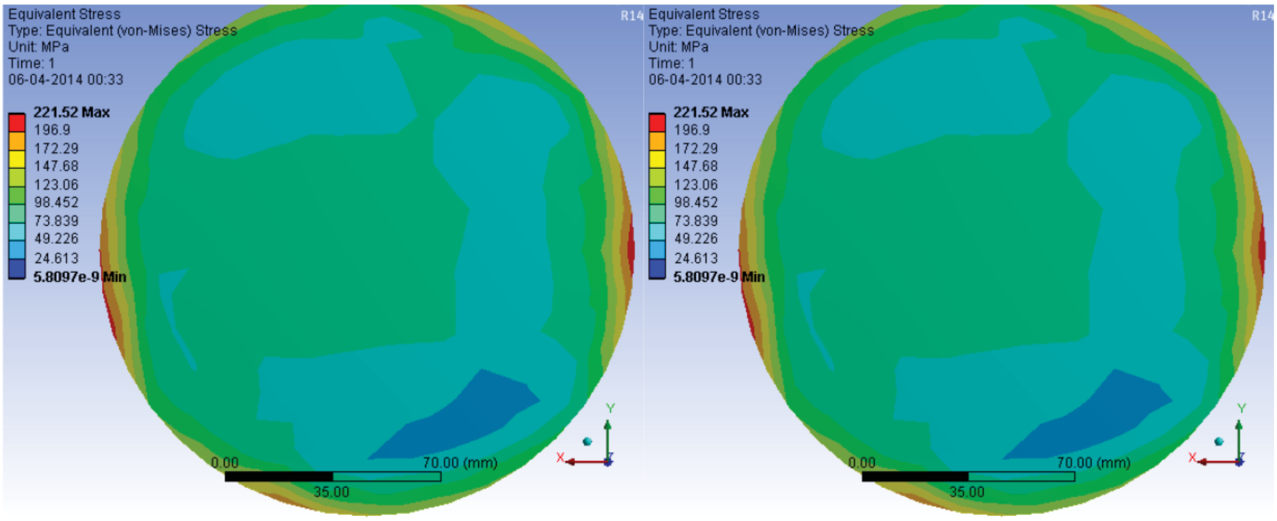

Fig. 8 Stress distribution in type II

Figs. 7 and 8 show temperature and stress distribution in type II pipe at the inner wall of the valve at 150 and 300 sec. A similar tendency of temperature profile is obtained in type II pipe model. But the effect of turbulent penetration increases rapidly by decreasing the vertical height of the safety injection pipe as shown in Fig. 8. In first 150 s, broader width of the maximum temperature zone is obtained as compared with type I model. But the width of the maximum temperature zone decreases with the greater time step, i.e. at 300 s. Particularly, ΔT_{max} of each model significantly exceeds the threshold temperature difference $\Delta T_{threshold}$ which may lead the valve to thermal fatigue. The concept of the threshold temperature difference is presented as:

$$\Delta T_{threshold} = 1.183 \times S_a / (K_3 \times E \times \alpha)$$

S_a and K_3 respectively represent the alternating fatigue stress amplitude at approximately $2.5*10^7$ and peak stress index described in ASME Sec. III. E and α represent the elastic modulus and thermal expansion coefficient at room temperature. ΔT_{max} of each model has a value similar to the threshold temperature difference, 47.5 K. Therefore, special attention should be paid to the turbulent penetration of the flow. Furthermore, in type II model, as shown in Fig. 8 magnitude of maximum stress has increased by decreasing its height as well as the maximum stress zone is obtained at both 9 o'clock and 3 o'clock position. In addition, the location of maximum stress also changes with the change in time and geometric features.

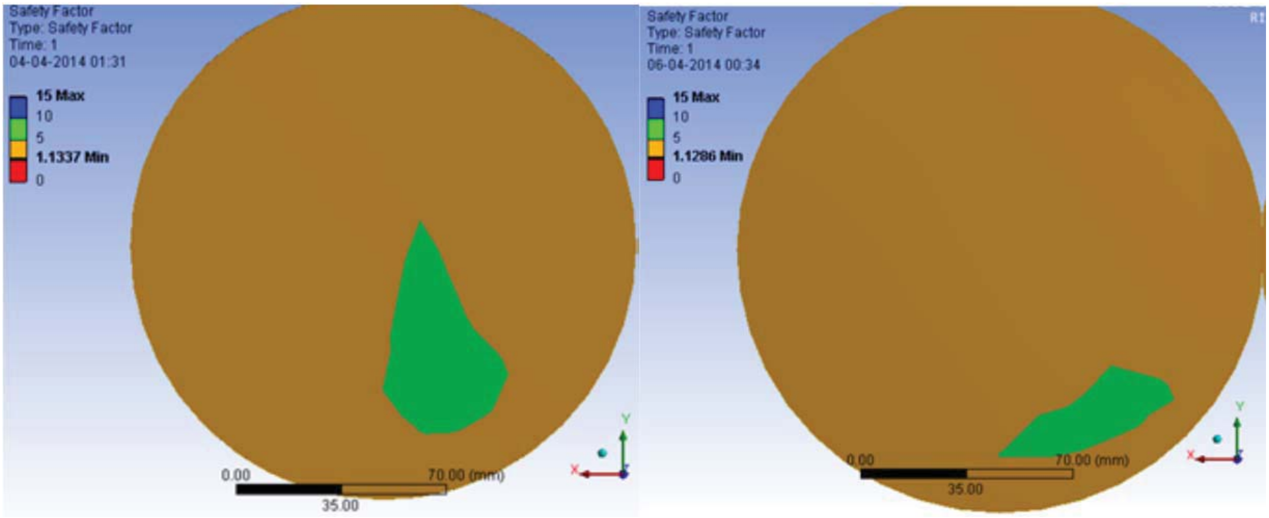

Fig. 9 Factor of safety for type I and type II

Minimum value of safety factor obtained among the different time steps has been taken for the analysis. The minimum factor of safety was obtained in type II model due to the fact that turbulent penetration has greater effect with the decrement of the vertical height of SIS pipe. Thus, type II model has to be the major concern of area. Furthermore, by comparing the data of each model, we can determine the trend in the change of the temperature according to the increment in time-step. Since the type II model has a greater turbulent penetration, higher temperatures are also developed in this model as compared with type I model.

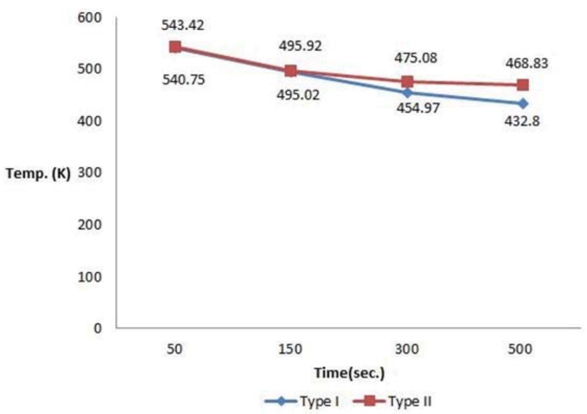

Fig. 10 Temperature trend of different model

V. Conclusion

Phenomenon of thermal stratification was simulated using ANSYS FLUENT with fixed mass flow rate. From the thermal analysis, the response characteristics of three types of SIS piping subjected to transient thermal stratification loadings were investigated. The main conclusions of this work are summarized as follows:

- As a step toward understanding the relationship between Von Mises stresses and turbulence, the peak stresses are generated because of rapid temperature change induced by turbulent penetration. However, since temperature changes are reduced when different temperature fluids mix, these stresses rapidly differ with time because of natural convection in the pipe.
- The two types of temperature profile in graph shows that the turbulence is considerably affected by the vertical pipe length. Initially, the temperatures are almost same for both the pipes but as the time precedes the temperature difference between the profiles increases which leads towards a consensus that flow is more turbulent in type II. Therefore, a valve leakage chance is less for longer vertical pipe.
- In addition, the location where maximum stress occurs changes with time according to the change in the temperature distribution. The maximum stress is obtained in type II pipe at 150 second on the rear side of the valve. By varying the length of the vertical pipe, we came to understand temperature and stress vary non-linearly but gradually increase with length of the vertical section and factor of safety being lowest for type II that is 1.1286 which verifies that it needs more maintenance than type I.
- By this analysis, we can specify that further cyclic thermal stress will lead to failure due to fatigue. Therefore, it is necessary to continuously perform the appropriate in-service inspection and evaluation on the stratified flow induced by turbulence penetration in the SIS piping [10].
- As future prospect, the phenomenon of thermal stripping can be considered in the computation. The valve critical leakage rate can be found out by using suitable software and the CFX-5 role and its usefulness in the design and analysis of the nuclear reactor lines are unsurpassable compared to FLUENT [11], [12].

References

[1] Klein, Dale E., and Dear Chairman Klein. "Subject: summary report-5491H meeting of the advisory committee on reactor safeguards, February 7-9, 2008, and other related activities of the committee." (2008).

[2] Kim, J. H., R. M. Roidt, and A. F. Deardorff. "Thermal stratification and reactor piping integrity." Nuclear Engineering and Design 139.1 (1993): 83-95.

[3] Coatsworth, Andrew M. and Nuclear Installations Inspectorate. "IAEA Annual Technical Committee Meeting of the INES National Officers IAEA Vienna 22-24 October 1997." (1997).

[4] Shah, VikramNaginbhai, et al. "Assessment of field experience related to pressurized water reactor primary system leaks." ASME publications-pvp395 (1999): 23-32.

[5] Agbadua, Segun, Afokhainu, et al. "Thermal Cycling Effects on the Fatigue Behaviour of Low Carbon Steel." Journal of Minerals and Materials Characterization and Engineering 10 (2011): 1345.

[6] Kim, Sunhye, et al. "A coupled cfd-fem analysis on the safety injection piping subjected to thermal stratification." Nuclear Engineering and Technology 45.2 (2013): 237-248.

[7] Ashgriz, Nasser, and Javad Mostaghimi. "An introduction to Computational Fluid Dynamics." Fluid flow handbook. McGraw-Hill Professional (2002).

[8] Tannehill, J.C., Anderson, D.A., and Pletcher, R.H., “Computatioal Fluid Mechanics and Heat Transfer,” Taylor & Francis, 1997.

[9] Pletcher, Richard H., John C. Tannehill, and Dale Anderson. Computational fluid mechanics and heat transfer. CRC Press, 2012.

[10] Nichols, Robert H., Robert W. Tramel, and P. G. Buning. "Solver and turbulence model upgrades to OVERFLOW 2 for unsteady and high-speed applications." AIAA paper 2824 (2006): 2006

[11] S. Chattopadhyay, “Structural evaluation of a piping system subjected to thermal stratification,” Nucl. Eng. & Design, Vol. 239, pp. 2236-2241 (2009).

[12] Verification and validation of a thermal stratification experiment CFD simulation by Hugo C. Regende – nuclear engineering and design, 248 (2012), pp. 72-81.